Inorg. Chem. **2004**, *43*, 6793–6804

Structures and Properties of Ruthenium(II) Complexes of Pyridylamine Ligands with Oxygen-Bound Amide Moieties: Regulation of Structures and Proton-Coupled Electron Transfer

Takahiko Kojima,* Ken-ichi Hayashi, and Yoshihisa Matsuda

Department of Chemistry, Faculty of Sciences, Kyushu University, Hakozaki, Higashi-Ku, Fukuoka 812-8581, Japan

Received April 2, 2004

Tris(2-pyridylemthyl)amine (TPA) derivatives having two amide moieties at the 6-positions of the two pyridine rings of TPA and their Ru(II) complexes were synthesized and characterized by spectroscopic methods, X-ray crystallography, and electrochemical measurements. The complexes prepared were $[RuCl(L)]PF_6$ (L = *N*,*N*-bis-(6-(1-naphthoylamide)-2-pyridylmethyl)-*N*-(2-pyridylmethyl)amine (**1**), *N*,*N*-bis(6-(2-naphthoylamide)-2-pyridylmethyl)-*N*-(2-pyridylmethyl)amine (**2**), *N*,*N*-bis(6-(isobutyrylamide)-2-pyridylmethyl)-*N*-(2-pyridylmethyl)amine (**3**)); the crystal structures of the three compounds were established by X-ray crystallography. In variable-temperature ^{1}H NMR spectra of **1** and **2** in CD_3CN solutions, the π–π stacking in **1** was too rigid to exhibit any fluxional motions in NMR measurements; however, the π–π stacking of **2** was weaker and showed fluxional behavior in nearly T-shaped π–π interaction for the 2-naphthly groups ($\Delta H^\circ = -2.3$ kJ mol^{-1}; $\Delta G^\circ = -0.9$ kJ mol^{-1} and $\Delta S^\circ = -7.7$ J mol^{-1} K^{-1} at 233 K in CD_3CN). For each of these three complexes, one of the amide moieties coordinated to the Ru(II) center through an amide oxygen. The other uncoordinated amide N–H formed intramolecular hydrogen bonding which remained intact even in aqueous media, indicating the intramolecular hydrogen bonding was geometrically compelled to form. The amide coordination is also stabilized and strengthened by the hydrogen bonding, so that the structure of each compound is maintained in solution. It is suggested that this hydrogen bonding lowers the redox potentials of the Ru(II) centers due to polarization of the coordinated amide C═O bond, in which the oxygen atom becomes more electrostatically negative and its electron-donating ability is strengthened. The N–H protons in the coordinated amide moieties were found to undergo a reversible deprotonation–protonation process, and the redox potentials of the Ru(II) centers could be regulated in the range of 500 mV in CH_3CN solutions. The Pourbaix diagram for **1** clearly showed that this proton-coupled redox behavior is a one-electron/one-proton process, and the pK_a value was estimated to be ~6.

Introduction

Amide linkage (−NHC(O)−) is known to be strong enough to form and maintain protein architectures which are appropriate to perform their missions in biological systems.[1] To form complex three-dimensional structures such as α-helix and β-sheet scaffolds, the amide moieties interact through hydrogen bonding in addition to noncovalent interactions among amino acid residues. The amide linkage has been utilized to create various molecular devices for a spectrum of purposes in organic chemistry. In the development of sophisticated molecular devices, functional moieties have been introduced via amide linkages, and multifunctional molecules can be formed by convergence of functional groups linked together via amide linkages.[2] The amide moiety

* Author to whom correspondence should be addressed. E-mail: cosyscc@mbox.nc.kyushu-u.ac.jp. Fax: +81-92-642-2570.

(1) Albert, B.; Bray, D.; Lewis, J.; Raff, M.; Roberts, K.; Watson, J. D. *Molecular Biology of the Cell*, 3rd ed.; Garland Publishing: New York, 1994; Chapter 3.

(2) (a) Frehill, F.; Vos, J. G.; Benrezzak, S.; Koós, A. A.; Kónya, Z.; Rüther, M. G.; Blau, W. J.; Fonseca, A.; Nagy, J. B.; Biró, L. P.; Minett, A. I.; in het Panhuis, M. *J. Am. Chem. Soc.* **2002**, *124*, 13694−13695. (b) Chang, S.-K.; Van Engen, D.; Fan, E.; Hamilton, A. D. *J. Am. Chem. Soc.* **1991**, *113*, 7640−7645. (c) Král, V.; Sessler, J. L.; Furuta, H. *J. Am. Chem. Soc.* **1992**, *114*, 8704−8705. (d) Askew, B.; Ballester, Buhr, C.; Jeong, K. S.; Jones, S.; Parris, K.; Williams, K.; Rebek, J., Jr. *J. Am. Chem. Soc.* **1989**, *111*, 1082−1090. (e) Rebek, J., Jr. *Acc. Chem. Res.* **1990**, *23*, 399−404; *Angew. Chem., Int. Ed. Engl.* **1990**, *29*, 245−255. (f) Nowick, J. S.; Feng, Q.; Tjivikua, T.; Ballester, P.; Rebek, J., Jr. *J. Am. Chem. Soc.* **1990**, *113*, 8831−8839.

10.1021/ic0495665 CCC: $27.50
Published on Web 09/22/2004

can also interact with metal ions as proposed in Fe(III)−enterobactin complexation.[3] Raymond and co-workers have postulated that the coordination of amide oxygen, concomitant with phenoxide of catechol moieties and its protonation−deprotonation, is important in the uptake and release of iron ion accompanied by its redox process.[4]

Regulation of environments around metal ions has been achieved by using ligands with amide-linked functional groups. As for transition metal complexes, such scaffolds have been used to build up specific hydrophobic or hydrophilic microenvironments[5] around metal binding sites for molecular recognition[6] and catalysis performed by metalloenzymes.[7] For instance, steric hindrance by pivaloylamide groups have been applied for "picket fence porphyrin" complexes as models of hemoglobin or myoglobin to protect the iron-bound dioxygen molecule from forming μ-oxo dimers and to stabilize dioxygen binding with intramolecular hydrogen bonding among the proximal metal-bound oxygen atom and amide N−H protons.[8] Those structural benefits have been effectively and intensively applied to non-heme environments by Masuda and co-workers. They have developed pivaloylamide-containing TPA (TPA = tris(2-pyridylmethyl)amine) ligands and have applied them to stabilize superoxo−[9] and hydroperoxo−Cu(II)[10] complexes and also hydroxo−[11] and alkylperoxo−Fe(III)[12] complexes. In their systems, the pivaloylamide group(s) acts both as a protective group and a hydrogen-binding site by N−H moieties, as in the case of "picket-fence porphyrins". Borovik and co-workers have also developed amide ligands to stabilize metal−oxo and −hydroxo species by virtue of intramolecular hydrogen bindings.[13]

In general, the amide linkage can be bound to a metal ion by one of the two coordination modes shown in Chart 1. In addition to the structural benefits mentioned above, another important utility of a coordinated amide moiety is regulation of the redox property of a metal ion. The amide binds through N^- to a metal ion in a deprotonated (amidate) form (form a in Chart 1) to stabilize unusual high-valent states of metal ions, such as Cu(III), Ni(III), Co(IV), Mn(V), and Fe(IV), as reported by Margerum,[14] Collins,[15] and co-workers. Such a structural motif has been proposed in Fe−bleomycin,[16] which activates dioxygen toward oxidative cleavage of DNA via the degradation of deoxyribose.[17] In addition, ligands containing the amidate coordination have been applied to asymmetric catalysis, for example, the allylic alkylation by palladium complexes with asymmetric amide−phosphine ligands reported by Trost and co-workers.[18]

Chart 1. Coordination Modes of Amide Linkage: (a) Deprotonated N-Coordination, (b) O-Coordination and Its Reversible Deprotonation−Protonation

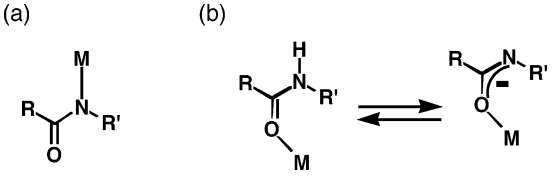

In contrast, oxygen-bound amides shown in Chart 1b have been reported for Cu(II)−peptide complexes under acidic conditions;[19] however, few crystal structures have been established.[20] In biological systems, metal ions in active sites having oxygen-bound amide moieties as ligands have been found in an iron-dependent regulator protein, which is one of the primary transcriptional regulators,[21] in isopenicillin

(3) Raymond, K. N.; Dertz, E. A.; Kim, S. S. *Proc. Natl. Acad. Sci. U.S.A.* **2003**, *100*, 3584−3588.
(4) Cohen, S. M.; Meyer, M.; Raymond, K. N. *J. Am. Chem. Soc.* **1998**, *120*, 6277−6286 and references therein.
(5) Sigel, H.; Martin, R. B. *Chem. Rev.* **1982**, *82*, 385−426.
(6) (a) Beer, P. D.; Timoshenko, V.; Maestri, M.; Passaniti, P.; Balzani, V. *Chem, Commun.* **1999**, 1755−1756. (b) Goodman, M. S.; Hamilton, A. D.; Weiss, J. *J. Am. Chem. Soc.* **1995**, *117*, 8447−8455. (c) Linton, B.; Hamilton, A. D. *Chem. Rev.* **1997**, *97*, 1669−1680 and references therein.
(7) Lippard, S. J.; Berg, J. M. *Principles of Bioinorganic Chemistry*; University Science Book: Mill Valley, CA, 1994.
(8) (a) Collman, J. P.; Gagne, R. R.; Halbert, T. R.; Marchon, J.-C.; Reed, C. A. *J. Am. Chem. Soc.* **1973**, *95*, 7868−7870. (b) Collman, J. P.; Gagne, R. R.; Reed, C. A.; Halbert, T. R.; Lang, G.; Robinson, W. T. *J. Am. Chem. Soc.* **1975**, *97*, 1427−1439. (c) Collman, J. P.; Brauman, J. I.; Doxsee, K. M.; Halbert, T. R.; Bunnenberg, E.; Linder, R. E.; LaMar, G. N.; Gaudio, J. D.; Lang, G.; Spartalian, K. *J. Am. Chem. Soc.* **1980**, *102*, 4182−4192. (d) Kim, K.; Fettinger, J.; Sessler, J. L.; Cyr, M.; Hugdahl, J.; Collman, J. P.; Ibers, J. A. *J. Am. Chem. Soc.* **1989**, *111*, 403−405.
(9) Harata, M.; Jitsukawa, K.; Masuda, H.; Einaga, H. *J. Am. Chem. Soc.* **1994**, *116*, 10817−10818. Tolman and co-workers have claimed that the complex was a hydroxo complex: Berreau, L. M.; Mahapatra, S.; Halfen, J. A.; Young, V. G., Jr.; Tolman, W. B. *Inorg. Chem.* **1996**, *35*, 6339−6342.
(10) Wada, A.; Harata, M. Hasegawa, K.; Jitsukawa, K.; Masuda, H.; Mukai, M.; Kitagawa, T.; Einaga, H. *Angew. Chem., Int. Ed.* **1998**, *37*, 798−799.
(11) Ogo, S.; Wada, A.; Watanabe, Y.; Iwase, M.; Wada, A.; Harata, M.; Jitsukawa, K.; Masuda, H.; Einaga, H. *Angew. Chem., Int. Ed.* **1998**, *37*, 2102−2104.
(12) Wada, A.; Ogo, S.; Watanabe, Y.; Mukai, M.; Kitagawa, T.; Jitsukawa, K.; Masuda, H.; Einaga, H. *Inorg. Chem.* **1999**, *38*, 3592−3593.
(13) (a) Gupta, R.; Borovik, A. S. *J. Am. Chem. Soc.* **2003**, *125*, 13234−13242. (b) Gupta, R.; MacBeth, C. E.; Young, V. G., Jr.; Borovik, A. S. *J. Am. Chem. Soc.* **2002**, *124*, 1136−1137. (c) MacBeth, C. E.; Hammes, B. S.; Young, V. G., Jr.; Borovik, A. S. *Inorg. Chem.* **2001**, *40*, 4733−4741. (d) MacBeth, C. E.; Golombek, A. P.; Young, V. G., Jr.; Yang, C.; Kuczera, K.; Hendrich, M. P.; Borovik, A. S. *Science* **2000**, *289*, 938−941.
(14) Margerum, D. W. *Pure Appl. Chem.* **1983**, *55*, 23−34.
(15) (a) Collins, T. J. *Acc. Chem. Res.* **2002**, *35*, 782−790. (b) Bartos, M. J.; Gordon-Wylie, S. W.; Fox, B. G.; Wright, L. J.; Weintraub, S. T.; Kauffmann, K. E.; Münck, E.; Kosta, K. L.; Uffelman, E. S.; Rickard, C. E. F.; Noon, K. R.; Collins, T. J. *Coord. Chem. Rev.* **1998**, *174*, 361−390. (c) Collins, T. J. *Acc. Chem. Res.* **1994**, *27*, 279−285.
(16) (a) Sugiura, Y. *J. Am. Chem. Soc.* **1980**, *102*, 5208−5215. (b) Crystal structure of Cu(II)−P3A: Iitaka, Y.; Nakamura, H.; Nakatani, T.; Muraoka, Y.; Fujii, A.; Takita, T.; Umezawa, H. *J. Antibiot.* **1978**, *31*, 1070−1072.
(17) Burger, R. M. *Chem. Rev.* **1998**, *98*, 1153−1169.
(18) (a) Trost, B. M.; Lee, C. B. *J. Am. Chem. Soc.* **2001**, *123*, 3671−3686. (b) Trost, B. M.; Crawley, M. *J. Am. Chem. Soc.* **2002**, *124*, 9328−9329. (c) Trost, B. M.; Dogra, K.; Hachiya, I.; Emura, T.; Hughes, D. L.; Krska, S.; Reamer, R. A.; Palucki, M.; Yasuda, N.; Reider, P. J. *Angew. Chem., Int. Ed.* **2002**, *41*, 1929−1932.
(19) (a) Sigel, H. *Inorg. Chem.* **1975**, *14*, 1535−1540. (b) Sigel, H.; Naumann, C. F.; Prijs, B.; McCormick, D. B.; Falk, M. C. *Inorg. Chem.* **1977**, *16*, 790−796. (c) El-Shazly, M. F.; El-Dissowky, Salem, T.; Osman, M. *Inorg. Chim. Acta* **1980**, *40*, 1−6.
(20) (a) Malval, J.-P.; Lapouyade, R. *Helv. Chim. Acta*, **2001**, 2439−2451. (b) Inoue, M. B.; Muñoz, I. C.; Machi, L.; Inoue, M.; Fernando, Q. *Inorg. Chim. Acta* **2000**, *311*, 50−56. (c) Bugella-Altamirano, E.; González-Pérez, J. M.; Sicilia Zafra, A. G.; Niclós-Gutiérrez, J.; Castiñeiras-Campos, A. *Polyhedron* **2000**, *19*, 2463−2471, 2473−2481. (d) Cornman, C. R.; Zovinka, E. P.; Boyajian, Y. D.; Olmstead, M. M.; Noll, B. C. *Inorg. Chim. Acta* **1999**, *285*, 134−137. (e) Adhikari, N.; Chaudhuri, S.; Butcher, R. J.; Saha, N. *Polyhedron* **1999**, *18*, 1323−1328. (f) Cini, R.; Intini, F. P.; Maresca, L.; Pacifico, C.; Natile, G. *Eur. J. Inorg. Chem.* **1998**, 1305−1312. (g) See also ref 4.
(21) Feese, M. D.; Ingason, B. P.; Goranson-Siekierke, J.; Holmes, R. K.; Hol, W. G. J. *J. Biol. Chem.* **2001**, *276*, 5959−5966.

N synthase,[22] and Ni^{2+}- and Co^{2+}-bound diphtheria toxin repressor.[23] Such a coordination mode of amide linkage will be useful for providing unique microenvironments and for regulating redox potentials of metal centers by altering the donating ability of the amide moiety in accordance with reversible deprotonation−protonation behavior as depicted in Chart 1b, without isomerization as observed in Cu(II)−peptide complexes.

We have investigated the synthesis and characterization of ruthenium−TPA complexes[24] and their reactivity toward catalytic hydrocarbon oxygenation.[25] In this article, we describe the synthesis and characterization of ruthenium complexes with bisamide-TPA derivatives with various hydrophobic groups. They exhibit interesting behavior in terms of intramolecular noncovalent interactions and redox control by deprotonation−protonation of a coordinated amide moiety. A part of this work has been reported previously.[26]

Experimental Section

Materials and Apparatus. CH_2Cl_2, CCl_4, and CH_3CN were distilled on CaH_2 under N_2 prior to use. Chemicals such as 1-naphthoyl chloride and 2-naphthoyl chloride were distilled and stored under N_2. *N*-Bromosuccinimide (NBS) was recrystallized from hot water prior to use. Other chemicals were used as received. *N*-Bis(6-pivaoylamide-2-pyridylmethyl)-*N*-(2-pyridylmethyl)amine was prepared as reported.[27] *cis*-$[RuCl_2(DMSO)_4]$ was synthesized according to literature methods.[28]

UV−vis absorption spectra were recorded on a Jasco Ubest-55 UV/vis spectrophotometer at room temperature. All NMR measurements were carried out on JEOL GX-400 and EX-270 spectrometers. Infrared spectra were recorded as KBr disks in the range of 4000−400 cm^{-1} on a Jasco IR model 800 infrared spectrophotometer. FAB-MS spectra were measured on a JMS-SX/SX102A tandem mass spectrometer. Elemental analysis data for all compounds were obtained at the Service Center of the Elemental Analysis of Organic Compounds, Department of Chemistry, Kyushu University.

Synthesis of *N*,*N*-Bis(6-bis(1-naphthoyl)amide)-2-pyridylmethyl)-*N*-(2-pyridylmethyl)amine ((1-Naph)$_4$-TPA). To an ice-cooled solution of *N*-bis(6-amino-2-pyridylmethyl)-*N*-(2-pyridylmethyl)amine (0.823 g, 2.57 mmol) and triethylamine (2 mL) in CH_2Cl_2 (20 mL) was added dropwise a solution of 1-naphthoyl chloride (2 mL, ca. 10 mmol) in CH_2Cl_2 (10 mL). After completion of the addition at 0 °C, the mixture was stirred at room temperature overnight. The white precipitate (triethylammonium chloride) was filtered off, and the filtrate was washed with 0.5 M aqueous Na_2CO_3, followed by water, and then dried on $MgSO_4$. Column chromatography on silica gel eluted by ethyl acetate ($R_f = 0.70$) gave (1-Naph)$_4$-TPA as a brown-white powder in 60% yield. Anal. Calcd for $C_{62}H_{45}N_6O_{4.5}$ ((1-Naph)$_4$-TPA·1/2H_2O): C, 78.71; H, 4.79; N, 8.88. Found: C, 78.43; H, 4.95; N, 8.58. ^{1}H NMR (CD_3CN): δ 3.01 (s, 2H, $-CH_2-$), 3.07 (s, 4H, $-CH_2-$), 7.1−8 (multiplets, aromatic), 8.23 (dd, 8 and 1 Hz, 4H, H2 of naph), 8.42 (d, 6 Hz, 1H, H6 of py). ^{13}C NMR ($CDCl_3$): δ 58.8 (CH_2-py), 59.8 (CH_2-py-1-naph), 136.2 (C4 of py), 138.3 (C4 of py-1-naph), 148.7 (C6 of py-1-naph), 152.3 (C6 of py), 159.1 (C2 of py), 159.6 (C5 of py-1-naph), 172.6 (>C=O). FAB-MS: *m*/*e* 938.14 ($[M + H]^+$).

Synthesis of *N*-Bis(6-bis(2-naphthoyl)amide)-2-pyridylmethyl)-*N*-(2-pyridylmethyl)amine ((2-Naph)$_4$-TPA). This compound was prepared as described above except 1.2 g (10 mmol) of 4-(dimethylamino)pyridine (DMAP) was added, and the mixture was stirred for 1 week at room temperature. The compound was purified on a silica gel column eluted with ethyl acetate ($R_f = 0.66$) to obtain it as a white solid in 40% yield. ^{1}H NMR ($CDCl_3$): δ 3.08 (s, 2H, CH_2-pyr), 3.20 (s, 4H, CH_2-(2-Naph$_2$-pyr), 6.8−7.8 (multiplets, aromatic), 8.35 (s, 4H, H1 of 2-naphthyl), 8.39 (d, J = 5 Hz, 1H, pyr-H6).

Synthesis of *N*-Bis(6-isobutyrylamide)-2-pyridylmethyl)-*N*-(2-pyridylmethyl)amine ((Isob)$_2$-TPA). This compound was synthesized by a procedure similar to that described above. To a solution of 6,6′-diamino-TPA·3HCl (1.0 g, 2.3 mmol) and NEt_3 (8 mL) in CH_2Cl_2 (40 mL) was added dropwise a solution of isobutyryl chloride in CH_2Cl_2 at 0 °C under N_2. The compound was purified on a silica gel column eluted by EtOAc. ^{1}H NMR ($CDCl_3$): δ 1.26 (d, 7 Hz, CH_3 of isobutyryl, 12H), 2.54 (7-tet, 7 Hz, C*H* of isobutyryl, 2H), 3.75 (s, CH_2-py-6-isob, 4H), 3.89 (s, CH_2-py, 2H), 7.16 (td, 5 and 1 Hz, H-5 of py, 1H), 7.26 (d, H-5 of py-6-isob, 2H), 7.54 (d, H-3 of py, 1H), 7.66 (t, 8 Hz, H-4 of py), 7.67 (t, 8 Hz, H-4 of py-6-isob), 7.87 (s, amide N−H, 2H), 8.09 (d, 8 Hz, H-3 of py-6-isob, 2H), 8.53 (d, 8 Hz, H-6 of py, 1H). HRMS: calcd for $\{C_{26}H_{32}N_6O_2 + H\}^+$, 461.5780; found, 461.2669.

Synthesis of *N*,*N*-Bis(6-amino-2-pyridylmethyl)-*N*-(5-methyl-2-pyridylmethyl)amine. A mixture of (5-methyl-2-pyridyl)-methylamine·HCl (0.857 g, 4.39 mmol) and 6-(pivaloylamide)-2-bromomethylpyridine (2.38 g, 8.79 mmol) was refluxed for 16 h in the presence of Na_2CO_3 (4.65 g, 43.9 mmol) in CH_3CN (70 mL). After filtration, the filtrate was dried under reduced pressure. The residue was washed with Et_2O, and the ligand *N*-bis(6-(pivaloylamide)-2-pyridylmethyl)-*N*-(5-methyl-2-pyridylmethyl)amine was obtained as a brown powder (2.18 g, 98% yield). This compound was converted to *N*,*N*-bis(6-amino-2-pyridylmethyl)-*N*-(5-methyl-2-pyridylmethyl)amine by hydrolysis with NaOH (2.08 g, 51.8 mmol) in EtOH/H_2O (5:2 v/v, 70 mL) through 24 h refluxing. Concentrated HCL was added to adjust the pH to <2. The mixture was filtered, and the filtrate was dried under reduced pressure. The residue was dissolved into EtOH and then filtered. The filtrate was dried to obtain the HCl salt of the compound (1.93 g, 99% yield). ^{1}H NMR (D_2O): δ 2.25 (s, 3H, $-CH_3$), 3.73 (s, 4H, $-CH_2-$ of NH_2-py), 3.82 (s, 2H, $-CH_2-$ of 5-CH_3-py) 6.61 (d, 2H, J = 8 Hz, H3 of NH_2-py, and d, 2H, J = 8 Hz, H5 of NH_2-py), 7.53 (t, 2H, J = 8 Hz, H4 of NH_2-py), 7.65 (d, 2H, J = 8 Hz, H3 of 5-Me-py), 8.08 (d, 2H, J = 8 Hz, H4 of 5-Me-py), 8.31 (d, 2H, J = 8 Hz, H6 of 5-Me-py). This material was used for the next step without further purification.

(22) Roach, P. L.; Clifton, I. J.; Hensgens, C. M. H.; Shibata, N.; Schofield, C. J.; Hajdu; Baldwin, J. E. *Nature* **1997**, *387*, 827−830.

(23) (a) White, A.; Ding, X.; vanderSpek, J. C.; Murphy, J. R.; Ringe, D. *Nature* **1998**, *394*, 502−506. (b) Pohl, E.; Holmes, R. K.; Hol, W. G. J. *J. Mol. Biol.* **1999**, *292*, 653−667.

(24) (a) Kojima, T. *Chem. Lett.* **1996**, 121−122. (b) Kojima, T.; Amano, T. Ishii, Y.; Ohba, M.; Okaue, Y.; Matsuda, Y. *Inorg. Chem.* **1998**, *37*, 4076−4085. (c) Kojima, T.; Matsuda, Y. *J. Chem. Soc., Dalton Trans.* **2001**, 958−960. (d) Kojima, T.; Sakamoto, T.; Matsuda, Y.; Ohkubo, K.; Fukuzumi, S. *Angew. Chem., Int. Ed.* **2003**, *42*, 4951−4954. (e) Kojima, T.; Sakamoto, T.; Matsuda, Y. *Inorg. Chem.* **2004**, *43*, 2243−2245. See also: (f) Koshi, C.; Umakoshi, K.; Sasaki, Y. *Chem. Lett.* **1997**, 1155−1156. (g) Bjernemose, J.; Hazell, A.; McKenzie, C. J.; Mahon, M. F.; Nielsen, L. P.; Rainthby, P. R.; Simonsen, O.; Toftlund, H.; Wolny, J. A. *Polyhedron* **2003**, *22*, 875−885.

(25) (a) Kojima, T.; Matsuda, Y. *Chem. Lett.* **1999**, 81−82. (b) Kojima, T.; Matsuo, H.; Matsuda, Y. *Inorg. Chim. Acta* **2000**, *300*−*302*, 661−667. (c) see also ref 24a and the following: Yamaguchi, M. Kousaka, H.; Yamagishi, T. *Chem. Lett.* **1997**, 769−770.

(26) Kojima, T.; Hayashi, K.; Matsuda, Y. *Chem. Lett.* **2000**, 1008−1009.

(27) (a) Harata, M.; Hasegawa, K.; Jitsukawa, K.; Masuda, H.; Einaga, H. *Bull. Chem. Soc. Jpn.* **1998**, *71*, 1031−1038. (b) See also ref 9b.

(28) James, B. K.; Ochiai, E.; Rempel, G. I. *Inorg. Nucl. Chem. Lett.* **1971**, *7*, 781−784.

Synthesis of *N*,*N*-Bis(6-bis(1-naphthoyl)amide)-2-pyridylmethyl)-*N*-(5-methyl-2-pyridylmethyl)amine (5-Me-(1-Naph)$_4$-TPA). To a degassed solution of *N*,*N*-bis(6-amino-2-pyridylmethyl)-*N*-(5-methyl-2-pyridylmethyl)amine·3HCl (1.00 g, 2.25 mmol) and NEt_3 (3.14 mL, 22.5 mol) in CH_2Cl_2 (40 mL) was added 1-naphthoyl chloride (1.7 mL, 11 mmol) in CH_2Cl_2 (10 mL) dropwise over a period of 30 min under N_2 at 0 °C. The mixture was stirred at room temperature and then filtered. The filtrate was dried up under reduced pressure and purified by column chromatography on silica gel eluted with AcOEt ($R_f = 0.75$). The ligand was obtained as a yellow solid (0.85 g, 40% yield). ^{1}H NMR ($CDCl_3$): δ 2.26 (s, 3H, 5-C*H*$_3$), 3.39 (s, 4H, C*H*$_2$− of 1-naph-py), 3.42 (s, 2H, C*H*$_2$ of 5-Me-py), 7−8.4 (multiplets, aromatic), 9.07 (d, 1H, $J = 8$ Hz, H6 of py). This material was used for the synthesis of complex **4** without further purification.

Synthesis of *N*-(6-(Bis(1-naphthoylamide)-2-pyridylmethyl)-*N*,*N*-bis(2-pyridylmethyl)amine. To an ice-cooled solution of *N*-(6-amino-2-pyridylmethyl)-*N*,*N*-bis(2-pyridylmethyl)amine (3.0 g, 9.8 mmol) in CH_2Cl_2 (200 mL) with NEt_3 (5 mL, 36 mmol) was added 1-naphthoyl chloride (3.0 mL, 20 mmol) in CH_2Cl_2 (20 mL) dropwise at 0 °C. The mixture was stirred at 0 °C and then warmed to room temperature while stirring overnight. After removal of the white precipitate by filtration, the filtrate was concentrated to a small volume and eluted on an alumina column with EtOAc/hexane/aqueous NH_3 (1:1:0.02) and then EtOAc/aqueous NH_3 (100:2). The final red fraction was collected and dried using a rotatory evaporator to obtain the ligand precursor.

Synthesis of [RuCl((1-Naph)$_2$-TPA)]PF$_6$·H$_2$O (1·H$_2$O). To a refluxed solution of $RuCl_3$·3H_2O (55.7 mg, 0.213 mmol) and H_2SO_4 (20.6 mg, 0.213 mmol) in ethanol (50 mL) was added (1-Naph)$_4$-TPA (200 mg, 0.213 mmol) as a solid, and the mixture was allowed to reflux for 24 h. To the resultant red solution was added $NaPF_6$ (42.6 mg, 0.256 mmol), and the solution was concentrated to a small volume to obtain an orange powder of **1**, which was washed with a minimum volume of EtOH and then washed well with diethyl ether (148 mg, 75% yield). Anal. Calcd for $C_{40}H_{32}N_6O_2ClRuPF_6$·$H_2O$: C, 51.75; H, 3.69; N, 9.05. Found: C, 51.78; H, 3.54; N, 8.92. ^{1}H NMR (CD_3CN): δ 4.33 and 4.49 (ABq, $J_{AB} = 18$ Hz, −C*H*$_2$−), 4.62 and 4.89 (ABq, $J_{AB} = 15$ Hz, −C*H*$_2$−), 4.69 and 5.27 (ABq, $J_{AB} = 14$ Hz, −C*H*$_2$−), 10.17 (s, amide N*H*). Absorption maxima (λ_{max} (nm), ϵ (M^{-1} cm^{-1})) in CH_3CN: 438 (br), 7.1×10^3; 283, 2.1×10^4.

This complex was also prepared by using [$RuCl_2(DMSO)_4$] as a starting material to react with the ligand in methanol at reflux in a comparable yield.

Synthesis of [RuCl((2-Naph)$_2$-TPA)]PF$_6$·H$_2$O (2·H$_2$O). This complex was synthesized as described above for **1**. The complex was obtained as an orange powder in 71% yield. Anal. Calcd for $C_{40}H_{32}N_6O_2ClRuPF_6$·$H_2O$: C, 51.75; H, 3.69; N, 9.05. Found: C, 51.53; H, 3.59; N, 9.22. ^{1}H NMR (CD_3CN): δ 4.27 and 4.52 (ABq, $J_{AB} = 18$ Hz, −C*H*$_2$−), 4.42 and 4.98 (ABq, $J_{AB} = 15$ Hz, −C*H*$_2$−), 4.66 and 5.20 (ABq, $J_{AB} = 14$ Hz, −C*H*$_2$−), 10.33 (s, amide N*H*) and 10.46 (s, amide N*H*). Absorption maxima (λ_{max} (nm), ϵ (M^{-1} cm^{-1})) in CH_3CN: 426 (br), 8.4×10^3; 280, 3.7×10^4.

Synthesis of [RuCl(Isob$_2$-TPA)]PF$_6$ (3) was done as described for that of **1**. The crude product was washed with MeOH to remove impurities. Yield: 26%. Anal. Calcd for $C_{26}H_{32}N_6O_2RuClPF_6$·$H_2O$: C, 41.09; H, 4.51; N, 11.06. Found: C, 41.57; H, 4.36; N: 11.22. ^{1}H NMR (CD_3CN): δ 1.18 (d, 7 Hz, C*H*$_3$ of isobutyryl), 1.25 (d, 7 Hz, C*H*$_3$ of isobutyryl), 1.35 (d, 7 Hz, C*H*$_3$ of isobutyryl), 1.43 (d, 7 Hz, C*H*$_3$ of isobutyryl), 2.81 (7-tet, 7 Hz, C*H* of isobutyryl), 3.02 (7-tet, 7 Hz, C*H* of isobutyryl), 4.18 and 4.37 (ABq, 18 Hz, −C*H*$_2$−), 4.54 and 4.84 (ABq, 15 Hz, −C*H*$_2$−), 4.56 and 5.18 (AXd's 14 Hz, −C*H*$_2$−), 6.95 (d, 8 Hz, H5-py-isob), 7.04−7.15 (overlap multiplet, aromatic), 7.51 (td, 8 and 1 Hz, H4 of py), 7.59 (t, 8 Hz, H4 of py-isob (uncoordinated)), 7.70 (t, 8 Hz, H4 of py-isob (coordinated)), 8.27 (d, 8 Hz, H5 of py-isob (coordinated)), 8.31 (d, 6 Hz, H6 of py), 9.45 (s, N−*H* of amide (uncoordinated and hydrogen-bonded)), 9.787 (s, N−*H* of amide (coordinated)).

Synthesis of [RuCl(5-Me-(1-Naph)$_2$-TPA)]PF$_6$·3H$_2$O (4·3H$_2$O). This complex was prepared in the same manner as **1**. The yield was 60%. ^{1}H NMR (CD_3CN): δ 4.29 and 4.46 (ABq, 2H, $J_{AB} = 17$ Hz, −C*H*$_2$−), 4.61 and 4.89 (ABq, $J_{AB} = 15$ Hz, 2H, −C*H*$_2$−), 4.69 and 5.28 (AXd, $J = 14$ Hz, 2H, −C*H*$_2$−), 6.341 (t, $J = 8$ Hz, naph-H6), 6.8−8.2 (multiplets, aromatic), 8.48 (d, $J = 9$ Hz, 1H, naph-H2). Anal. Calcd for $C_{41}H_{34}N_6O_2ClRuPF_6$·3$H_2O$: C, 50.34; H, 4.12; N, 8.59. Found: C, 50.08; H, 3.87; N, 8.36.

X-ray Crystallography of 1. A single crystal of **1** was obtained by recrystallization from a methanol solution of **1** with Et_2O-vapor deposition. A red prismatic crystal ($0.25 \times 0.15 \times 0.25$ mm^3) was mounted on a glass fiber, and all measurements were made on a Rigaku AFC-7R diffractometer at 23 ± 1 °C with graphite-monochromated Mo Kα radiation ($\lambda = 0.7107$ Å). Cell constants and an orientation matrix for data collection were obtained from a least-squares refinement using the setting angles of 25 carefully centered reflections in the range of $29.54° < 2\theta < 29.96°$. The data collection was made with the $\omega-2\theta$ scan method to $2\theta_{max} = 55.1°$. Three standard reflections were monitored after every 150 reflections, and the standards increased by 1.2%. A linear correction was applied to the data to account for this phenomenon. Data were corrected for Lorentz−polarization effects and for absorption through azimuthal scans. A correction for secondary extinction was applied.

The structure was solved by direct methods and expanded using Fourier techniques. All non-hydrogen atoms were refined anisotropically. Refinement was carried out with full-matrix least-squares on *F* with scattering factors from reference and included anomalous dispersion effects. All calculations were performed using teXsan crystallographic software package.[29] The atomic scattering factors were taken from ref 30 and anomalous dispersion effects were included; the values for $\Delta f'$ and $\Delta f''$ were taken from ref 31. Disorder of a counteranion PF_6^- was observed. The hydrogen atoms were located at the calculated positions ($d = 0.95$ Å) and included in the final least-squares refinement.

X-ray Crystallography of 2·2H$_2$O. A single crystal of **2**·2H_2O was obtained by recrystallization from a CH_2Cl_2/EtOH solution. An orange prismatic crystal ($0.20 \times 0.20 \times 0.40$ mm^3) was mounted on a glass fiber. All measurements were made on a Rigaku RAXIS-RAPID imaging plate diffractometer with graphite-monochromated Mo Kα ($\lambda = 0.7107$ Å). Indexing was performed from 2 oscillations which were exposed for 3.3 min. The data were collected at −170 ± 1 °C to a maximum 2θ value of 55.0°. Data were processed by the PROCESS-AUTO program package. A symmetry-related absorption correction was applied, and the data were corrected for Lorentz−polarization effects.

The structure was solved by direct methods and expanded using Fourier techniques. All non-hydrogen atoms were refined aniso-

(29) *teXsan: Crystal Structure Analysis Package*; Molecular Structure Corp.: The Woodlands, TX, 1985 and 1999.
(30) Cromer, D. T.; Waber, J. T. *International Tables for X-ray Crystallography*; Kynoch Press: Birmingham, England, 1974; Vol. IV, Table 2.2A.
(31) *International Tables for X-ray Crystallography*; Kluwer Academic Publishers: Boston, MA, 1992; Vol. C.

Scheme 1. Synthesis of Ligands

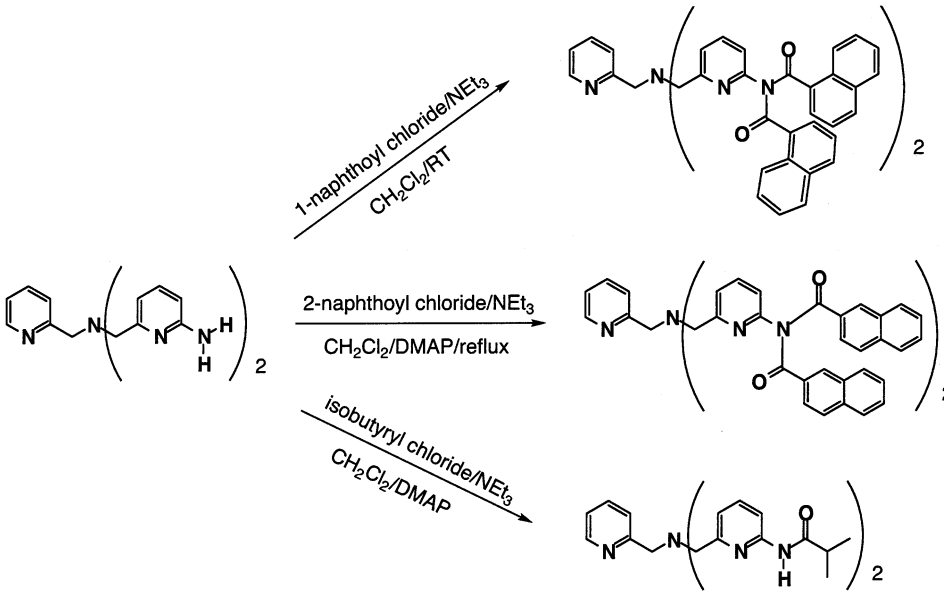

tropically by SHELXL-97,[32] and hydrogen atoms were included but not refined. The atomic scattering factors were taken from ref 30, and anomalous dispersion effects were included as mentioned above. Water molecules of crystallization were found to be disordered into two directions (O4 and O5, for which populations were set to be 0.5 for each atom). All calculations were performed using the teXsan crystallographic software package.

X-ray Crystallography of 3. Single crystals of **3** suitable for X-ray analysis were obtained by recrystallization from methanol. An orange platelet crystal of **3** ($0.03 \times 0.14 \times 0.19$ mm^3) was mounted on a glass fiber. All measurements were made on a Rigaku RAXIS-RAPID imaging plate diffractometer with graphite-monochromated Mo Kα ($\lambda = 0.7107$ Å) radiation. Indexing was performed from 3 oscillations, which were exposed for 3.0 min. The data were collected at -140 ± 1 °C to a maximum 2θ value of 55.0°. Data were processed by the PROCESS-AUTO program package. A symmetry-related absorption correction was applied, and the data were corrected for Lorentz−polarization effects.

The structure was solved by direct methods and expanded using Fourier techniques. All non-hydrogen atoms were refined anisotropically, and hydrogen atoms were included but not refined. The atomic scattering factors were taken from ref 30, and anomalous dispersion effects were included as mentioned above. All calculations were performed using the teXsan crystallographic software package.

Cyclic Voltammetry. All cyclic voltammograms were recorded on a HECS 312B dc pulse polarograph (Fuso Electrochemical System attached to a HECS 321B potential sweep unit of the same manufacture. A platinum disk (3 mm o.d.) was employed as a working electrode, a platinum coil as a counter electrode, and a silver/silver nitrate ($Ag/AgNO_3$) electrode as a reference electrode, respectively. All measurements were carried out in CH_3CN containing 0.1 M $[(n\text{-}Bu)_4N]ClO_4$ as a supporting electrolyte under N_2 at ambient temperatures. The redox potentials were determined relative to a ferrocene/ferrocenium couple as a reference (0 V).

Pourbaix diagrams were obtained by measurements of $E_{1/2}$ values in accordance with pH titration by 0.2 M NaOH aqueous solutions in CH_3CN/Britton−Robinson buffer (1:1 v/v) mixture at room temperature. The "apparent" pH values of this mixture are referred to as pH.

DFT Calculations on Model Complexes. Model complexes, $[RuCl(6,6'\text{-bis(acetoamide)-TPA})]^+$ and $[RuCl(6\text{-acetoamide-TPA})]^+$, were constructed on the basis of the atomic coordinates of **3**. DFT calculations were performed at the B3LYP/LANL2DZ level of theory.[33]

Results and Discussion

Synthesis. The ligands were synthesized on the basis of procedures for preparation of 6-pivalamide-TPA derivatives reported by Masuda and co-workers. Ligands employed here were synthesized by acylation of diamino-TPA, which was obtained by hydrolysis of 6,6′-bis(pivalamide)-TPA by NaOH in EtOH, with 1-naphthoyl, 2-naphthoyl, or isobutyryl chlorides in CH_2Cl_2 in the presence of base such as NEt_3. Synthetic routes are summarized in Scheme 1. In the case of 2-naphthoyl chloride, 10 equiv of 4-(dimethylamino)-pyridine (DMAP) was required in addition to NEt_3 and a much longer reaction time was needed to complete the amide formation. The compounds obtained were tetraamide derivatives for both naphthoyl chlorides, and they were used for the preparation of ruthenium complexes. Corresponding diamido-TPA ligands could be obtained by the solvolysis of the tetraamides of naphthyl derivatives in MeOH in the presence of Na_2CO_3; however, the purification was unsuccessful due to severe adsorption onto silica gel. Stoichiometric reaction of diamino-TPA with 1- or 2-naphthoyl chloride to obtain $(1\text{-naph})_2$-TPA or $(2\text{-naph})_2$-TPA gave a mixture of several species, so this procedure did not seem to be a reasonable synthetic procedure. The yields of ruthenium complexes from the reactions using diamide-TPA

(32) Sheldrick, G. M. *SHELXL-97, Program for the Refinement of Crystal Structures*; University of Göttingen: Göttingen, Germany, 1997.

(33) (a) Becke, A. D. *Phys. Rev. A* **1988**, *38*, 3098−3100. (b) Becke, A. D. *J. Chem. Phys.* **1993**, *98*, 5648−5652. (c) Lee, C.; Yang, W.; Parr, R. G. *Phys. Rev. B* **1988**, *37*, 785−789. (d) Dunning, T. H., Jr.; Hay, P. J. In *Modern Theoretical Chemistry*; Schaefer, H. F., III, Ed.; Plenum: New York, 1976. (e) Hay, P. J.; Wadt, W. R. *J. Chem. Phys.* **1985**, *82*, 299−310.

Table 1. Crystallographic Data for $[RuCl((1\text{-Naph})_2\text{-TPA})]PF_6$ (**1**), $[RuCl((2\text{-Naph})_2\text{-TPA})]PF_6 \cdot 2H_2O$ (**2**·$2H_2O$), and $[RuCl((Isob)_2\text{-TPA})]PF_6$ (**3**)

	1	**2**·$2H_2O$	**3**
empirical formula	$C_{40}H_{32}N_6O_2ClRu$ PF_6	$C_{40}H_{36}N_6O_4$ $ClRuPF_6$	$C_{26}H_{32}N_6O_2Cl$ $RuPF_6$
fw	910.22	946.25	742.07
cryst system	monoclinic	triclinic	monoclinic
space group	$P2_1/n$	$P\bar{1}$	$P2_1/c$
a, Å	16.253(2)	13.3675(5)	28.9965(1)
b, Å	13.756(2)	14.3432(7)	11.7893(2)
c, Å	17.874(2)	10.0746(6)	29.0517(1)
α, deg		98.118(2)	
β, deg	111.165(9)	93.159(3)	162.6539(4)
γ, deg		92.832(2)	
V, Å^3	3726.7(8)	1906.2(2)	2960.93(8)
Z	4	2	4
D_{calc}, g/cm^3	1.622	1.657	1.665
μ(Mo Kα), cm^{-1}	6.12	6.05	7.48
T, °C	23	−170	−140
no. of observns	4368 ($I > 3\sigma(I)$)	6575 (all data)	6793 (all data)
no. of variables	551	541	388
R	0.062	0.072	0.072
R_w	0.064	0.128	0.100
R_1	*a*	0.041 ($I > 2\sigma(I)$)	0.038 ($I > 2\sigma(I)$)
GOF	2.21	0.89	1.10

[a] Not available.

derivatives were almost the same as those of tetraamides, suggesting such solvolysis did not interfere with the formation of Ru(II) complexes. In the case of $Isob_2$-TPA, the reaction of diamino-TPA with an excess amount of isobutyryl chloride gave the diamide form as a main product in the presence of NEt_3 and 0.5 equiv of DMAP in CH_2Cl_2.

The ^{1}H NMR spectrum of $(1\text{-Naph})_4$-TPA in $CDCl_3$ showed two singlets at 3.33 and 3.31 ppm (intensity ratio of 1:2) assigned to the methylene moieties and no signals ascribed to amide N−H. That of $(2\text{-Naph})_4$-TPA also showed two singlets at 3.09 and 3.21 ppm (intensity ratio of 1:2) due to the methylene protons. As for $Isob_2$-TPA, those signals were observed at 3.89 and 3.75 ppm (intensity ratio of 1:2) and a broad singlet due to the amide N−H's was observed at 7.87 ppm. As for $Isob_2$-TPA, a doublet assigned to the methyl protons of the isopropyl groups was observed at 1.26 ppm ($J = 7$ Hz) and a 7-tet due to the methane proton of the isopropyl groups at 2.54 ppm ($J = 7$ Hz). Two singlets (intensity ratio of 1:2) ascribed to the methylene protons were observed at 3.89 and 3.75 ppm, which were downfield-shifted compared with the two mentioned above. In the case of $(1\text{-Naph})_4$-5-Me-TPA, a singlet due to the 5-methyl group was observed at 2.23 ppm and singlets assigned to the methylene protons were observed at 3.42 and 3.39 ppm (intensity ratio of 1:2).

Mononuclear Ru(II) complexes having $(1\text{-Naph})_2$-TPA and $(2\text{-Naph})_2$-TPA, $[RuCl((1\text{-Naph})_2\text{-TPA})]PF_6$ (**1**) and $[RuCl((2\text{-Naph})_2\text{-TPA})]PF_6$ (**2**), and $[RuCl(Isob_2\text{-TPA})]PF_6$ (**3**) were prepared by the reaction of $Ru^{III}Cl_3 \cdot 3H_2O$ with $(1\text{-Naph})_4$-TPA, $(2\text{-Naph})_4$-TPA, and $Isob_2$-TPA, respectively, in MeOH or EtOH. Interestingly, these reactions involve reduction of the ruthenium ion probably by alcohol, although the mechanism is presently not clear. The reactions proceeded smoothly, and complexes **1** and **2** were obtained in good yields. Reaction of $[RuCl_2(DMSO)_4]$ with the tetraamides gave the same complexes in similar yields. In the case of **3**, the yield was lower than those of the other two complexes, decreasing to 26%. To improve the yield, methanol was used as a solvent instead of EtOH and the yield improved up to ∼90% based on $RuCl_3 \cdot 3H_2O$. The addition of NEt_3 to the EtOH solution also improved the yield of **3**, but the main product obtained was revealed to be $[RuCl(Isob_2\text{-TPA}^-)]$, in which one of the amide protons was deprotonated (vide infra). This deprotonated species was easily converted to **3** by adding an acid such as HPF_6. The complex **4** with 5-Me-$(1\text{-Naph})_2$-TPA was also prepared in the same manner as those of **1** and **2** in 60% yield.

Molecular Structures of 1−3. X-ray crystallography on **1**−**3** was performed to determine their molecular structures. Their structures exhibited the following common features: (1) One amide oxygen coordinates to the Ru(II) center to form an asymmetric coordination environment. (2) The coordinated amide oxygen forms intramolecular hydrogen bonding with the uncoordinated amide N−H proton. (3) Two 6-amide-pyridine moieties are located trans to each other on the ruthenium center. The compound **1** was crystallized in monoclinic space group $P2_1/c$ having no solvent molecule of crystallization (Table 1). An ORTEP drawing of the cation moiety of **1** is shown in Figure 1, and selected bond lengths and angles are listed in Table 2. The Ru(II) center is a distorted octahedron possessing a chloride, a tertiary amino group, three pyridine nitrogens, and the amide oxygen of one of naphthoylamide moieties, indicating that the ligand acts as a pentadentate ligand. The two pyridine rings having the 6-(1-naphthoylamide) groups were located trans to each other, and the nonsubstituted pyridine was trans to the chloride. The coordinated amide oxygen was trans to the tertiary amino group. The environment around the ruthenium center is asymmetric due to the amide coordination. The configuration of this complex was asymmetric, and two enantiomers existed in the unit cell. The two amide-substituted pyridine rings were located on positions trans to each other. The coordinated amide oxygen O1 was found to form an intramolecular hydrogen bonding with the free

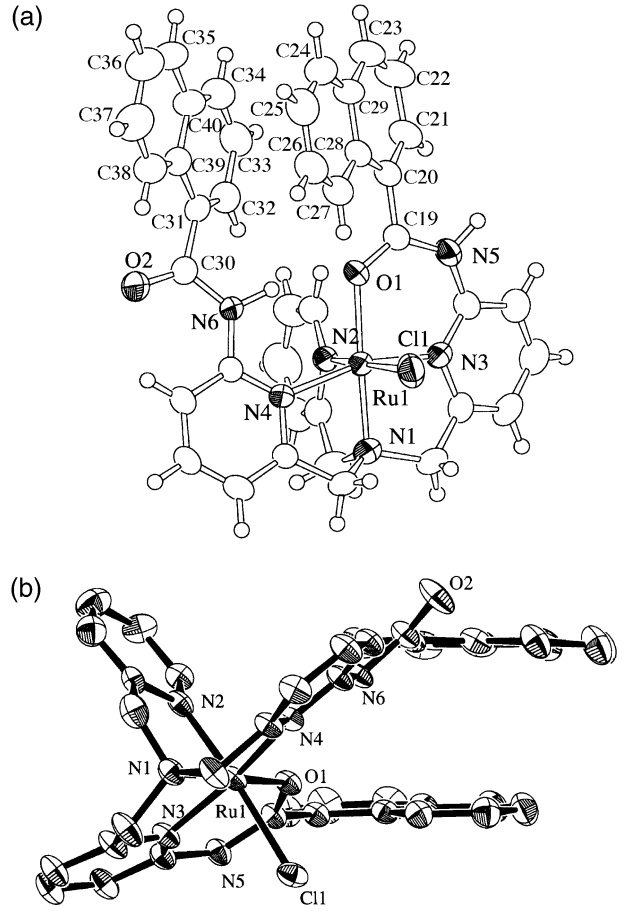

Figure 1. ORTEP drawing of cation moiety of **1** with 50% probability thermal ellipsoids: (a) overview; (b) side view. All hydrogen atoms were omitted for clarity in (b).

Table 2. Selected Bond Lengths (Å) and Angles (deg) for **1** and **2**·H_2O·1/2C_2H_5OH

	1	**2**·2H_2O		**1**	**2**·2H_2O
Ru1−Cl	2.446(2)	2.4351(9)	O1−C19	1.256(7)	1.261(4)
Ru1−O1	2.091(4)	2.105(2)	O2−C30	1.219(8)	1.223(4)
Ru1−N1	2.052(5)	2.055(3)	N5−C19	1.365(8)	1.366(4)
Ru1−N2	2.004(5)	2.059(3)	N6−C30	1.381(8)	1.377(4)
Ru1−N3	1.992(5)	2.005(3)	N5−C12	1.398(8)	1.403(4)
Ru1−N4	2.125(5)	2.113(3)	N6−C18	1.401(8)	1.397(4)
O1−Ru1−N3	90.4(2)	89.84(9)	O1−C19−C20	119.7(6)	118.7(3)
N1−Ru1−N2	81.8(2)	82.2(1)	N5−C19−C20	116.0(6)	117.0(3)
N1−Ru1−N3	85.4(2)	85.6(1)	C19−N5−C12	131.4(6)	132.3(3)
N1−Ru1−N4	80.0(2)	80.0(1)	O2−C30−N6	123.2(6)	122.9(3)
Cl1−Ru1−N2	175.9(2)	175.51(7)	O2−C30−C31	123.0(6)	122.2(3)
O1−Ru1−N1	173.6(2)	174.0(1)	N6−C30−C31	113.7(6)	114.8(3)
N3−Ru1−N4	165.3(2)	164.6(1)	C18−N6−C30	126.2(5)	126.5(3)
O1−C19−N5	124.2(6)	124.3(3)			

amide N(6)−H having 3.036(6) Å separation for O1···N6. This type of intramolecular hydrogen bonding has not been reported for Cu− and Fe−6-pivalamide-TPA complexes in which amide N−H's have been reported to form intramolecular hydrogen bonding rather with axial anion ligands such as OH^-, O_2^-, and OOH^- to stabilize those interesting structures.[9−12,27] This type of hydrogen bonding has been often observed in the β-sheet structure for protein folding.[34]

The ruthenium center possesses a distorted octahedral geometry having −N3−Ru1−N4 = 165.3(2)°, which is slightly larger than those observed for other Ru(II)−TPA complexes

Table 3. Selected Dihedral Angles (deg) for **1**−**3**

	1	**2**	**3**
Py(N3)−amide (coord)	13.4	10.4	8.7
amide (coord)−Naph	39.3	20.6	
Py(N4)−amide (uncoord)	4.3	20.7	8.2
amide (uncoord)−Naph	45.6	20.0	
Naph−Naph	5.9	27.1	

such as $[RuCl(TPA)]_2(ClO_4)_2$, $[RuCl(TPA)(DMSO)]PF_6$, and $[RuCl(5\text{-}Me_3\text{-}TPA)(DMSO)]ClO_4$. Unlike other Ru−TPA complexes, the bond lengths for Ru−N3 and Ru−N4 which are trans to each other are fairly different, 1.992(5) Å for Ru1−N3 and 2.125(5) Å for Ru1−N4. The bond distance for Ru1−O1 was 2.091(4) Å. This coordination can be accommodated by charge polarization of the C═O moiety due to the intramolecular hydrogen bonding as mentioned above, and such polarization can give the bond length of 1.256(7) Å longer than that of the uncoordinated C═O bond (1.219(8) Å). This effect will be further discussed in the section on electrochemical measurements. The dihedral angles between the pyridine rings and the amide moieties showed that the coordinated amide group (13.4°) was more distorted than the uncoordinated counterpart (4.3°). Dihedral angles to be discussed are summarized in Table 3. In contrast, the naphthalene plane was less rotated in the coordinated naphthalene arm having the dihedral angle of 39.3° against the amide plane than that of the uncoordinated part (45.6°). Essentially, the two naphthalene planes were parallel to show a calculated dihedral angle between the two naphthalene planes of 5.9° and to have an intramolecular $\pi-\pi$ stacking with the separation of ca. 3.4 Å, for which the shortest contact was 3.36(1) Å for C29−C34 (see Figure 1b).[35]

Compound **2** was crystallized in triclinic space group $P\bar{1}$ having one water molecule and 1/2 molecule of ethanol as solvent molecules of crystallization, which were confirmed by elemental analysis. An ORTEP drawing of the cation moiety of **2** is shown in Figure 2, and selected bond lengths and angles are summarized in Table 2. The geometry around the Ru(II) center is almost identical with that of **1** having pentadentate $(2\text{-Naph})_2$-TPA including one coordinated amide C═O group, which interacts with the uncoordinated amide N−H through a stronger intramolecular hydrogen bonding (N6···O1, 2.977(3) Å) than that found in **1**. As observed in **1**, the bond length of the coordinated C═O bond (1.261(4)Å) was longer than that of the uncoordinated counterpart (1.223(4) Å). Dihedral angles in 6-(2-naphthoylamide)-pyridyl moieties were calculated to be 10.4 and 20.7° between pyridine rings and amide planes in coordinated and uncoordinated ones, respectively, and 20.6 and 20.0° for amide-naphthalene planes in the same manner, as listed in Table 3. The dihedral angle between the two naphthalene planes was determined to be 27.1°, which is much larger than that in **1** and suggests that an intramolecular $\pi-\pi$ interaction is close to a T-shape (edge-to-face) interaction[36]

(34) (a) Smith, C. K.; Regan, L. *Acc. Chem. Res.* **1997**, *30*, 153−161. (b) Schneider, J. P.; Kelly, J. W. *J. Am. Chem. Soc.* **1995**, *117*, 2533−2546.

(35) (a) Hunter, C. A.; Sanders, J. K. M. *J. Am. Chem. Soc.* **1990**, *112*, 5525−5534. (b) Janiak, C. *J. Chem. Soc., Dalton Trans.* **2000**, 3885−3896.

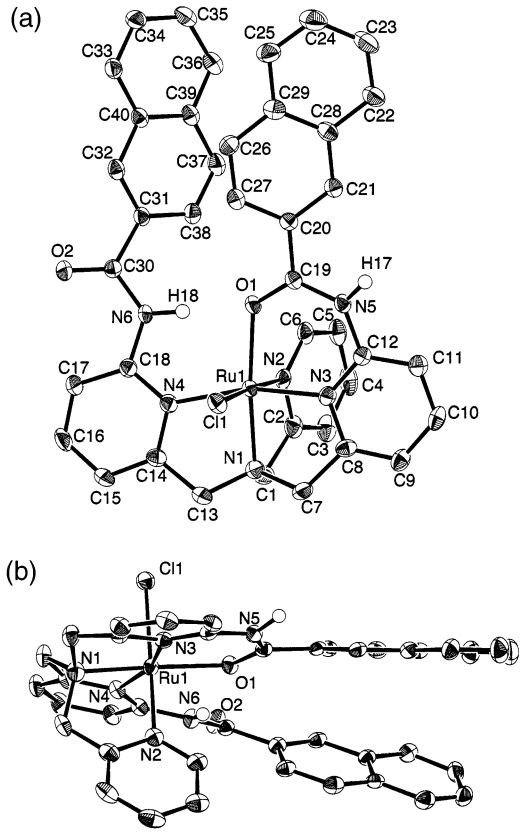

Figure 2. ORTEP representation of cation moiety of **2** with 50% probability thermal ellipsoids: (a) overview; (b) side view. All hydrogen atoms except amide hydrogen atoms were omitted for clarity.

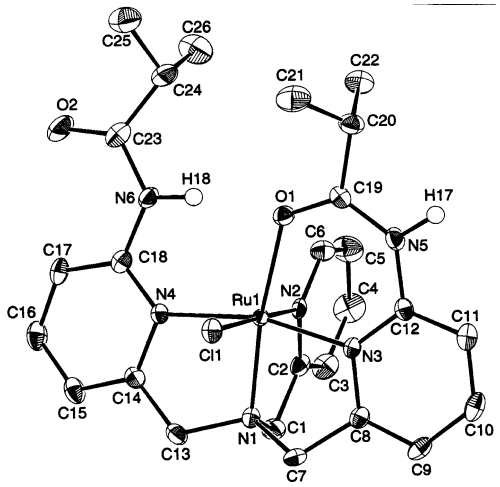

Figure 3. ORTEP drawing of cation moiety of **3** with 50% probability thermal ellipsoids. All hydrogen atoms except amide protons were omitted for clarity.

with the shortest contact of 3.395(5) Å for C27−C38 and weaker than that in **1** (see Figure 2b).

The crystal structure of **3** was determined, and an ORTEP drawing of the cation moiety is shown in Figure 3. Selected bond lengths (Å) and angles (deg) are listed in Table 4. The structural features are almost the same as those found in **1** and **2**. Intramolecular hydrogen bonding between the coordinated amide oxygen and the uncoordinated amide N−H moiety was also observed with N6···O1 distance of 3.041(6) Å. The coordinated amide N−H also formed strong hydrogen bonding with the counteranion PF_6^- (N5···F5, 2.925(4) Å). The dihedral angle between the mean pyridine plane containing N3 and the coordinated amide plane was determined to be 8.7(3)°, and that between the pyridine plane containing N4 and the uncoordinated amide plane was 8.2(3)°.

Table 4. Selected Bond Lengths (Å) and Angles (deg) for **3**

Ru1−Cl1	2.437(1)	Ru1−O1	2.117(3)
Ru1−N1	2.054(3)	Ru1−N2	2.031(3)
Ru1−N3	2.011(3)	Ru1−N4	2.126(3)
O1−C19	1.257(4)	O2−C23	1.217(5)
N5−C19	1.362(5)	N6−C23	1.387(5)
N5−C12	1.403(5)	N6−C18	1.392(5)
O1−Ru1−N3	90.6(1)	N1−Ru1−N2	82.7(1)
N1−Ru1−N3	83.4(1)	N1−Ru1−N4	88.8(1)
Cl1−Ru1−N2	178.18(9)	O1−Ru1−N1	172.9(1)
N3−Ru1−N4	164.4(1)	O1−C19−N5	125.0(4)
O1−C19−C20	119.8(3)	N5−C19−C20	115.2(3)
C19−N5−C12	133.0(3)	O2−C23−N6	123.1(4)
O2−C23−C24	122.5(4)	N6−C23−C24	114.3(3)
C18−N6−C23	127.8(3)		

On the basis of the fact that complex **3** is in the same structural motif around the ruthenium center as those of **1** and **2**, the intramolecular $\pi-\pi$ interaction as observed in **1** and **2** is not the determining factor for the geometry around the ruthenium center. Rather, the intramolecular hydrogen bonding is indispensable to form the asymmetric coordination environment involving the coordination of one amide oxygen atom. We assume that the intramolecular hydrogen bonding observed in **1**−**3** is not a result from the usual electrostatic interaction between an amide oxygen and an amide N−H moiety but is rather a stereochemically compelled one, and therefore, this hydrogen bonding is stable even in aqueous solution.

Spectroscopic Characterization of 1−3 in Solution. The ^{1}H NMR spectrum of **1** in CD_3CN showed that the six methylene protons were all unequivalent and were observed as three AB quartets. This is indicative of the asymmetric environment of **1** due to the coordination of the amide C═O group even in acetonitrile solution. Significant upfield shifts were observed for the naphthalene protons, especially for naph-H6 (6.39 ppm), suggesting that the $\pi-\pi$ stacking structure is also maintained in solution, as observed in the crystal structure. Variable-temperature ^{1}H NMR measurements in CD_3CN in the range from 60 to −40 °C showed no significant change to suggest that the metal-bound amide carbonyl group is not released within this temperature range even in the presence of >10 equiv of 4-methylpyridine as a potential ligand.

In the ^{1}H NMR spectrum of **2** in CD_3CN, the six methylene protons were also all unequivalent and were observed as three AB quartets as in those of **1**. In contrast to those of **1**, no peaks show such an upfield shift as observed in those of **1**. This suggests that the intramolecular $\pi-\pi$ interaction is not operating in **2** in solution at room temperature. In the variable-temperature ^{1}H NMR measurements for **2** in the range from −40 to 50 °C in CD_3CN, however, we could observe the dynamic motion of the 2-naphthyl moieties of **2**. As can be seen in Figure 4, one

(36) Jennings, W. B.; Farrell, B. M.; Malone, J. F. *Acc. Chem. Res.* **2001**, *34*, 885−894.

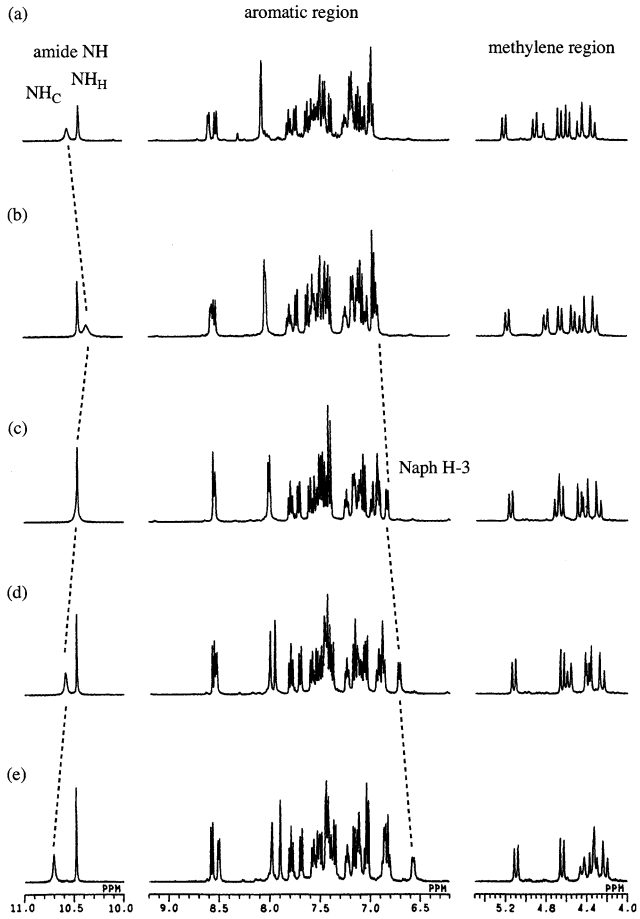

Figure 4. Variable-temperature ^{1}H NMR spectra of **2** in CD_3CN: (a) 40 °C; (b) 20 °C; (c) 0 °C; (d) −20 °C; (e) −40 °C. NH_C represents the amide proton of coordinated amide linkage, and NH_H stands for that involved in hydrogen bonding.

doublet exhibited an upfield shift and it was assignable to a naphthyl H-3, the closest hydrogen to the other naphthalene moiety to be most shielded by the ring current (see Figure 2b). This observation clearly shows that **2** has some flexibility in the motion of the naphthoyl moiety in solution. In contrast, **1** shows no fluxional behavior in $\pi-\pi$ stacking of the two 1-naphthyl groups. This is due to the difference of the intrinsic dihedral angle between naphthoyl group and amide plane; the 2-naphthoyl group has less steric hindrance in terms of rotation around the carbonyl group than the 1-naphthoyl group because of the lack of the peri-hydrogen. This observation clearly indicates that fluxional behavior of the intramolecular $\pi-\pi$ interaction is operating in complex **2**. The chemical shifts of several peaks showed linear relationships relative to $1/T$, indicating the mode of fluxional behavior of the intramolecular $\pi-\pi$ interaction in **2** should be unique.

Analysis of the temperature-dependent change of equilibrium constants was based on the arguments proposed by Johnson and Bovey[37] and those by Odani and Yamauchi.[38] We could obtain a good linear relationship between the stacking equilibrium constant (K) and $1/T$ as shown in Figure 5. On the basis of this relationship, thermodynamic parameters for the interaction were estimated to be $\Delta H° = -2.3$ kJ·mol^{-1}; therefore, $\Delta G° = -0.9$ kJ·mol^{-1} and $\Delta S° = -7.7$ J·mol^{-1}·K^{-1} at 233 K in CD_3CN.

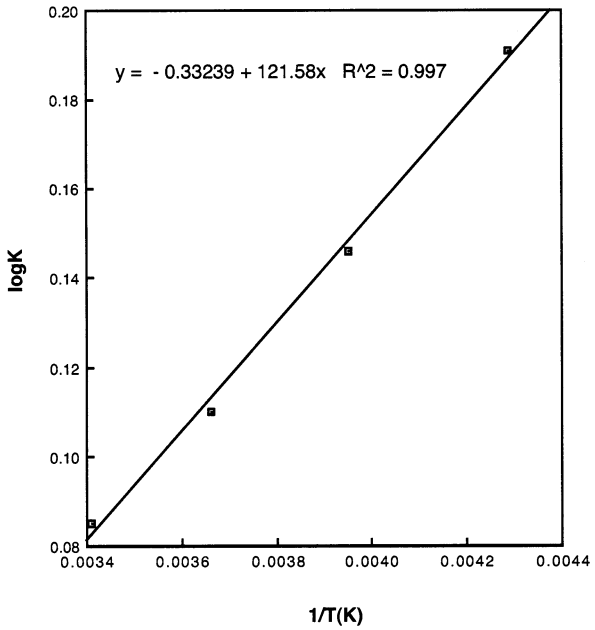

Figure 5. Temperature-dependence of equilibrium constants for the intramolecular $\pi-\pi$ interaction in **2**.

In the ^{1}H NMR spectra of **1** and **2** in CD_3CN, peaks assigned to the amide N−H hydrogen nuclei were observed and those peaks diminished slowly upon addition of an aliquot of D_2O, at 10.17 ppm for **1** as a tail-broadened singlet due to the overlap of two signals and two singlets at 10.33 and 10.46 ppm for **2**. As for those of **2**, the singlet at 10.33 ppm was broad and the other was fairly sharp and the broad peak diminished faster than the sharp one by adding D_2O. In addition, as can be seen in Figure 4, the sharp signal showed little change in its chemical shift; in contrast, the broad signal showed significant change of the chemical shift.[39] We assigned the broad signal to the chelated amide N−H on the basis of the stronger acidity and the sharp one to the uncoordinated amide N−H, which is involved in the intramolecular hydrogen bonding. The difference of the rate of H−D exchange is ascribed to the stronger acidity of the chelating amide N−H proton compared to the uncoordinated and hydrogen-bonded amide N−H. In the case of **3**, the N−H protons were observed as two clearly separated singlets at 9.45 and 9.79 ppm, which were assigned to the N−H of the hydrogen-bonded and uncoordinated amide moiety and that of the coordinated amide moiety, respectively. The singlet at 9.79 ppm was not observed in the deprotonated species [RuCl(Isob$_2$-TPA$^-$)], which was prepared in the presence of NEt_3, and the peak emerged upon addition of HPF_6 to give **3**. This suggests that the deprotonation and protonation of the N−H of the coordinated amide moiety should be reversible as described below.

(37) Johnson, C. E., Jr.; Bovey, F. A. *J. Chem. Phys.* **1958**, *29*, 1012−1014.
(38) Odani, A.; Deguchi, S.; Yamauchi, O. *Inorg. Chem.* **1986**, *25*, 62−69.
(39) In the case of **3**, the temperature-dependence of the chemical shift of N−H group was shown to be 1 ppb/K for the hydrogen-bonded N−H group (see Supporting Information).

Table 5. Redox Potentials for Ru^{II}/Ru^{III} Couples of **1**−**3** and Their Related Ru−TPA Complexes in CH_3CN at Room Temperature under N_2 (0.1 M TBAP)[a]

complex	$E_{1/2}$ (V)
[RuCl(1-Naph$_2$-TPA)]PF_6 (**1**)	0.34
[RuCl(2-Naph$_2$-TPA)]PF_6 (**2**)	0.30
[RuCl(Isob$_2$-TPA)]PF_6 (**3**)	0.27
1 + NEt_3	−0.16
2 + NEt_3	−0.15
3 + NEt_3	−0.21
[RuCl(TPA)(DMSO)]ClO_4	0.61[b]
[RuCl(5-Me$_3$-TPA)(DMSO)]ClO_4	0.52[b]
[Ru(TPA)(μ-Cl)]$_2$(ClO_4)$_2$	0.22 ($Ru^{II}Ru^{II}/Ru^{II}Ru^{III}$)[b]
	0.71 ($Ru^{II}Ru^{III}/Ru^{III}Ru^{III}$)[b]
[Ru(5-Me$_3$-TPA)(μ-Cl)]$_2$(ClO_4)$_2$	0.17 ($Ru^{II}Ru^{II}/Ru^{II}Ru^{III}$)[b]
	0.66 ($Ru^{II}Ru^{III}/Ru^{III}Ru^{III}$)[b]

[a] Potentials were determined relative to that of the ferrocene/ferrocenium redox couple as 0 V. [b] Reference 24b.

The two isopropyl groups in **3** were revealed to be unequivalent to show four doublets at 1.18, 1.25, 1.35, and 1.43 ppm and two methine protons at 2.81 and 3.02 ppm. Among them, the former two doublets were coupled with the 7-tet at 2.81 ppm and the latter two doublets were coupled with the other 7-tet at 3.02 ppm, as indicated by the $^1H-^1H$ COSY spectrum of **3**. This clearly indicates that one of isobutyrylamide moieties coordinates to the Ru(II) center as observed in **1** and **2**.

In the IR spectra of **1**−**3** obtained by the Nujol method, peaks assigned to the N−H stretching vibration were observed at 3314 cm^{-1} for **1**, 3335 cm^{-1} for **2**, and 3335 cm^{-1} for **3**, respectively. The two N−H stretching vibrations should be observed for both N−H bonds in the coordinated amide moieties and the hydrogen-bonded ones; however, those two probably overlapped to give one peak, suggesting the two different N−H bonds could have similar bond strengths. Those values were lower than those for typical N-substituted amide N−H (3450−3500 cm^{-1}), supporting the existence of the intramolecular hydrogen bonding.[40]

Electrochemical Measurements. Cyclic voltammograms of **1**−**3** were measured in CH_3CN in the presence of 0.1 M of [(*n*-butyl)$_4$N]ClO_4 (TBAP) as an electrolyte under N_2. Redox potentials were determined relative to ferrocene/ferrocenium (Fc/Fc^+) as 0 V. Redox potentials discussed in this paper are summarized in Table 5, together with those of related complexes. The complex **1** showed a reversible redox wave due to the Ru(II)/Ru(III) redox couple at $E_{1/2}$ = +0.34V vs ferrocene/ferrocenium redox couple as a reference. That of **2** was observed at +0.30 V, which was slightly lower than that of **1**. The complex **3** showed a reversible redox wave at $E_{1/2}$ = 0.27 V. Those potentials are much lower than those of mononuclear $[RuCl(L)(DMSO)]^+$ complexes (L = TPA and 5-Me_3-TPA). This may be due to strong coordination of the amide C═O moieties which should be polarized by the intramolecular hydrogen bonding as shown in Chart 2. This effect should be reflected on the longer bond lengths of C═O bonds of the coordinated amide parts than those of the uncoordinated ones.

Chart 2

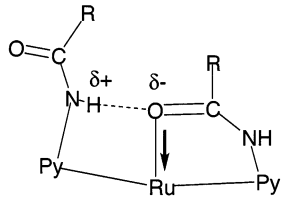

To clarify this electronic effect of the intramolecular hydrogen bonding between the coordinated amide oxygen and the uncoordinated amide N−H proton, we evaluated the change of Mulliken charges of coordinated amide oxygen atoms and ruthenium centers in model complexes by DFT calculations at the B3LYP/LANL2DZ level of theory (see Supporting Information).[41] The results of the calculations showed an increased negative Mulliken charge on the coordinated amide oxygen (−0.332) with the hydrogen bonding compared with that (−0.279) without such hydrogen bonding. The Mulliken charge of the Ru center was also influenced by the intramolecular hydrogen bonding; it was estimated to be +0.397 for the model with it and +0.420 for the model without it. These results indicate that the intramolecular hydrogen bonding toward the coordinated amide oxygen renders the Ru(II) center less positive and lowers its redox potential. This tendency exhibits sharp contrast to the cases of Mo(V) complexes having *o*-(acylamino)benzenethiolates, in which intramolecular hydrogen bonding between the coordinated sulfur atom and amide N−H moiety contribute to the positive shift of Mo(V)/Mo(IV) redox potentials.[42] In this case, the negative charge on the metal-bound thiolate sulfur atom should be compensated by the intramolecular hydrogen bonding to induce the positive shift. The present case is unique in this aspect; that is, the intramolecular hydrogen bonding polarizes the coordinated C═O moiety to render the oxygen more negative and it causes the negative shift of the redox potential of the ruthenium center.

In the cyclic voltammogram of **1**, in addition to the Ru^{II}/Ru^{III} redox couple mentioned above, we could observe a reduction process of the coordinated naphthoylamide moiety at −0.76 V and concomitant generation of a new reversible redox couple at −0.03 V. The reduction of the uncoordinated naphthoylamide moiety was also observed at

(40) Pimentel, G. C.; McClellan, A. L. *The Hydrogen Bond*; Reinhold Publishing: New York, 1960; p 307.

(41) (a) Becke, A. D. *Phys. Rev. A.* **1988**, *38*, 3098−3100. (b) Becke, A. D. *J. Chem. Phys.* **1993**, *98*, 5648−5652. (c) Lee, C.; Yang, W.; Parr, R. G. *Phys. Rev. B* **1988**, *37*, 785−789. (d) Dunning, T. H., Jr.; Hay, P. J. In *Modern Theoretical Chemistry*; Schaefer, H. F., III, Ed.; Plenum: New York, 1976. (e) Hay, P. J.; Wadt, W. R. *J. Chem. Phys.* **1985**, *82*, 299−310.

(42) Ueyama, N.; Okamura, T.; Nakamura, A. *J. Am. Chem. Soc.* **1992**, *114*, 8129−8137. (b) Ueyama, N.; Okamura, T.; Nakamura, A. *J. Chem. Soc., Chem. Commun.* **1992**, 1019−1020. (c) Ueno, T.; Ueyama, N.; Nakamura, A. *J. Chem. Soc., Dalton Trans.* **1996**, 3859−3863. (d) Ueno, T.; Inohara, M. Ueyama, N.; Nakamura, A. *Bull. Chem. Soc. Jpn.* **1997**, *70*, 1077−1083. (e) Ueno, T.; Kousumi, Y.; Yoshizawa-Kumagaye, K.; Nakajima, K.; Ueyama, N.; Okamura, T.; Nakamura, A. *J. Am. Chem. Soc.* **1998**, *120*, 12264−12273. (f) Ueyama, N.; Nishikawa, N.; Yamada, Y.; Okamura, T.; Nakamura, A. *Inorg. Chim. Acta* **1998**, *283*, 91−97. (g) Okamura, T.; Takamizawa, S.; Ueyama, N.; Nakamura, A. *Inorg. Chem.* **1998**, *37*, 18−28. (h) Ueyama, N.; Nishikawa, N.; Yamada, Y.; Okamura, T.; Oka, S.; Sakurai, H.; Nakamura, A. *Inorg. Chem.* **1998**, *37*, 2415−2421.

Scheme 2. Reversible Deprotonation−Protonation Behavior of **1**−**3**

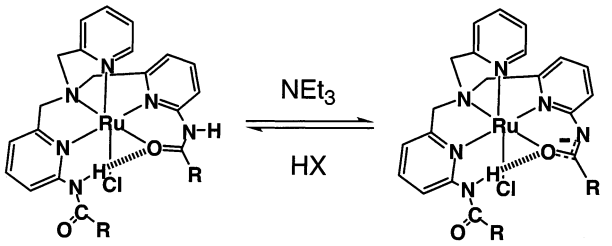

−1.45 V, which was comparable to that of 2-(1-naphthoylamide)-6-picoline (−1.43 V).

Reversible Deprotonation−Protonation of the N−H Proton of the Coordinated Amide To Control the Redox Potentials of Ruthenium Centers. As mentioned above, the oxygen of the coordinated amide group should bind to the ruthenium center and its coordination is enhanced by the intramolecular hydrogen bonding. This strong interaction will result in the reduction of electron density in the amide moiety and make the N−H proton more acidic than that of the uncoordinated and hydrogen-bonded counterpart. Thus, we discovered its facile deprotonation by the addition of NEt_3 and its recovery by the addition of $HClO_4$ or HPF_6 in CH_3CN.[43] A schematic description of this reversible deprotonation−protonation behavior is presented in Scheme 2.

In the UV−vis spectra of **1** and **2** in CH_3CN, we observed LMCT bands at 438 and 426 nm, respectively. Those LMCT bands are thought to involve charge transfers from Cl^- to Ru(II) center and, probably, from the coordinated amide C=*O* to the metal center. In the case of **1**, the original absorption spectrum is shown in Figure 6 as trace a. Upon addition of 2 aliquots of NEt_3, its absorptions at 438 nm with shoulder around 400 nm were converged into one larger absorption at 459 nm as shown in Figure 6 (trace b) and the $\pi-\pi^*$ transition of pyridines of TPA was also shifted from 284 to 291 nm. The red shift of the LMCT band from the coordinated amide oxygen to the metal center indicates that the deprotonation elevates the energy level of orbitals of the amide moiety, and this is consistent with the assignment. Following addition of $HClO_4$ recovered the original spectrum of **1** as depicted in the figure (trace c). This clearly indicates the complete reversibility of the protonation−deprotonation of the coordinated amide N−H.

As for **3**, we could observe such behavior in the ^1H NMR spectrum in CD_3CN. As described above, the broad singlet due to the N−H proton of the coordinated amide moiety was observed at 9.79 ppm and the uncoordinated and hydrogen-bonded one were observed at 9.45 ppm, respectively. Upon addition of an excess amount (>10 equiv) of NEt_3, the peak at 9.79 ppm disappeared and the other peaks were almost intact. At this stage, no significant spectral change was observed except a slight upfield shift of a doublet probably assignable to the H-5 proton of the pyridine ring with the coordinated amide arm. It is surprising that the deprotonation does not affect so much the chemical shifts of all other resonances. The addition of one aliquot of HPF_6 (60%) also recovered the original spectrum of **3**. These results suggest that the coordinated amide oxygen is already fairly negative in its character by virtue of the intramolecular hydrogen bonding.

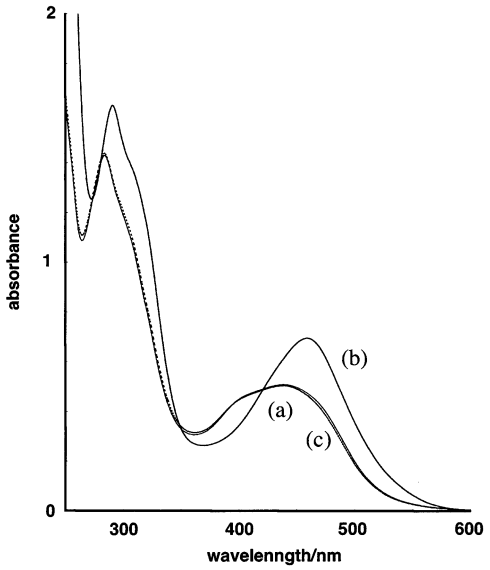

Figure 6. UV−vis spectral change for **1** in CH_3CN: (a) original; (b) addition of 2 aliquots of NEt_3; (c) (b) + 2 aliquots of $HClO_4$ (70%) (dotted line).

Influence of this reversible deprotonation−protonation behavior of the complexes **1**−**3** was examined by means of electrochemical measurements. The CV of **3** in CH_3CN, as described above, showed a reversible redox wave at $E_{1/2}$ = 0.27 V, assigned to the Ru(II)/Ru(III) redox couple. In sharp contrast to that, upon addition of an excess amount of NEt_3, the CV was completely changed to show a reversible redox wave at −0.21 V, which was 0.48 V lower than that of the original potential of **3**. The other two complexes showed similar behavior, and those potentials were drastically changed toward negative potentials as depicted in Table 5. Thus, the deprotonation at the amide N−H could control the redox potentials of those related complexes.

To confirm the mechanism of this proton-coupled electron-transfer process, we examined pH-dependence of the redox potential of the ruthenium center for **1** in CH_3CN/Britton−Robinson buffer (1:1 v/v) by a 0.2 M NaOH aqueous solution at room temperature in the "apparent pH" range of 1.72−9.28. At higher pH, the deprotonated form of **1** precipitated due to being electronically neutral and thus hardly dissolving in aqueous media. The resultant Pourbaix diagram is shown in Figure 7. The gradient of the linear relationship between pH and $E_{1/2}$ for Ru(II)/Ru(III) redox couple was determined to be −51.4 mV/pH, suggesting this process is a one proton−one electron process. We were unable to determine the accurate pK_a value for this process due to precipitation of the deprotonated species from the aqueous buffer solution. Apparent pK_a value is estimated to be ∼6 for **1** on the basis of the Pourbaix diagram. Comparison of the value with other reported pK_a values of amide N−H moieties indicates that the amide is much more acidic than free amides (pK_a ∼ 15).[44]

(43) Masuda and co-workers have reported that O-coordinated amide N−H could be deprotonated in a Cu(II) coordination sphere: Harata, M.; Jitsukawa, K.; Masuda, H.; Einaga, H. *Bull. Chem. Soc. Jpn.* **1998**, *71*, 637−645.

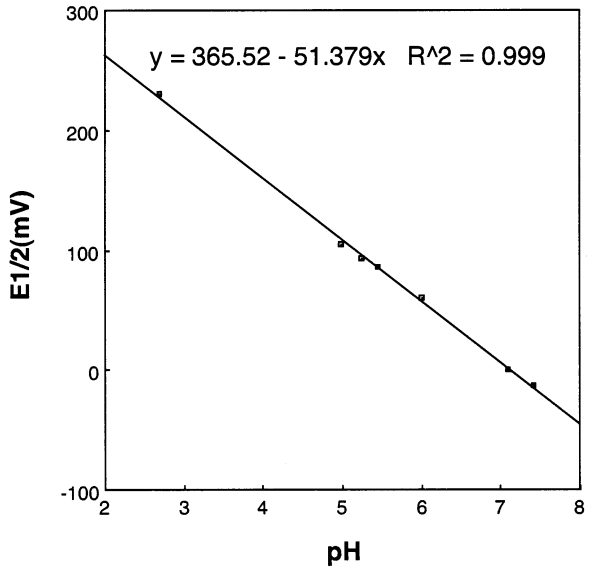

Figure 7. Pourbaix diagram for the titration of **1** in CH_3CN/Britton−Robinson buffer (1:1 v/v) mixture at room temperature.

Thus, the reversible deprotonation-protonation of the coordinated amide N−H can drastically control the redox potentials of the ruthenium center in the range of ∼500 mV.

Proton-dependent changes of redox potentials of metal complexes have been reported.[45] Haga and co-workers have reported that ruthenium complexes having benzimidazole-containing chelating ligands undergo reversible deprotonation−protonation processes to exhibit PCET changing redox potentials of the ruthenium centers in the range of ∼300 mV.[46] Recently, Brewer and co-workers have reported on PCET and spin state regulation in iron complexes with tripodal imidazole ligands, in which PCET allowed the exhibit of redox potential control in a range of ca. 300 mV.[47] These ranges of alteration of the redox potentials are smaller than those observed for **1**−**3**. In contrast, drastic change of redox potentials have been observed in *trans*-$[Ru(2,2'\text{-bipyridyl})_2(OH_2)_2]^{2+}$, for which the Ru(II)/Ru(III) redox potential has been altered in the range ∼500 mV.[48] Thus, the deprotonation−protonation of the coordinated amide N−H is comparable to that of metal-bound aqua ligand in terms of regulation of the redox potential of metal center.

Conclusion

We have synthesized and characterized a series of Ru(II) complexes with bisamide-TPA derivatives as ligands. Those complexes had intramolecular hydrogen bonding between coordinated amide oxygen and uncoordinated amide N−*H* to stabilize the structures and to lower the redox potential of Ru(II)/Ru(III) redox couple. The coordinated amide linkage undergoes reversible deprotonation−protonation (Scheme 1) with $pK_a \sim 6$ to regulate the redox potential of the Ru^{II}/Ru^{III} redox couple in the range of 500 mV without structural change. The complex having naphthyl groups exhibited intramolecular $\pi-\pi$ interaction which was differentiated between 1-naphthyl groups and 2-naphthyl ones; the 1-naphthyl derivative showed no fluxional motion and rigidity of the structure, and the 2-naphthyl one exhibited fluxional behavior for the interaction.

Acknowledgment. This work was supported by Grants-in-Aid (Nos. 09740495 and 11740373 to T.K.) from the Ministry of Science, Technology, Culture, and Education of Japan and a grant from Nissan Science Foundation (T.K.). We also appreciate Drs. Masaaki Ohba (Department of Chemistry, Kysuhu University), Mikio Yasutake, and Yuichi Shimazaki (Institute for Materials Chemistry and Engineering, Kyushu University) for their help in X-ray crystallography and Dr. Yoshihito Shiota and Prof. Kazunari Yoshizawa (Institute for Materials Chemistry and Engineering, Kyushu University) for their performing DFT calculations. We also thank Ms. Kayoko Ogi (Kyushu University) for her assistance in VT-NMR spectroscopy. Finally, T.K. is grateful to Prof. Christin T. Choma (Rensselaer Polytechnic Institute, Troy, NY) for her help in editing the manuscript.

Supporting Information Available: Crystallographic data for **1**−**3** in CIF format, model complexes for DFT calculations and Mulliken charges of each atom, and temperature-dependence of chemical shifts of N−H nuclei of **3** in ^1H NMR spectra. This material is available free of charge via the Internet at http://pubs.acs.org.

IC0495665

(44) Molday, R. S.; Kallen, R. G. *J. Am. Chem. Soc.* **1972**, *94*, 6739−6745.
(45) Slattery, S. J.; Blaho, J. K.; Lehnes, J.; Goldsby, K. A. *Coord. Chem. Rev.* **1998**, *174*, 391−416 and references therein.
(46) (a) Bond, A. M.; Haga, M. *Inorg. Chem.* **1986**, *25*, 4507−4514. (b) Haga, M.; Ano, T.; Kano, K.; Yamabe, S. *Inorg. Chem.* **1991**, *30*, 3843−3849. (c) Haga, M.; Ano, T.; Ishizaki, T.; Kano, K.; Nazaki, K.; Ohno, T. *J. Chem. Soc., Dalton Trans.* **1994**, 263−272.
(47) Brewer, C.; Brewer, G.; Luckett, C.; Marbury, G. S.; Viragh, C.; Beatty, A. M.; Scheidt, W. R. *Inorg. Chem.* **2004**, *43*, 2402−2415.
(48) Dobson, J. C.; Meyer, T. J. *Inorg. Chem.* **1988**, *27*, 3283−3291.